Korean J. Chem. Eng., **30**(2), 369-378 (2013)
DOI: 10.1007/s11814-012-0127-8

Batch and continuous (fixed-bed column) biosorption of Cu(II) by *Tamarindus indica* fruit shell

Shamik Chowdhury† and Papita Das Saha

Department of Biotechnology, National Institute of Technology-Durgapur,
Mahatma Gandhi Avenue, Durgapur 713209, West Bengal, India
(*Received 2 April 2012 • accepted 5 August 2012*)

Abstract−The feasibility of employing *Tamarindus indica* (tamarind) fruit shell (TFS) as low-cost biosorbent for removal of Cu(II) from aqueous solutions was investigated. Batch experiments were carried out as function of initial solution pH (2-7), contact time (10-240 min), initial Cu(II) concentration (20-100 mg L^{-1}), biosorbent dose (0.5-5 g) and temperature (293-313 K). Biosorption equilibrium data were well described by the Langmuir isotherm model with maximum biosorption capacity of 80.01 mg g^{-1} at 313 K. Biosorption of Cu(II) followed pseudo-second-order kinetics. Gibbs free energy (ΔG^0) was spontaneous for all interactions, and the biosorption process exhibited endothermic enthalpy values. To ascertain the practical applicability of the biosorbent, fixed-bed column studies were also performed. The breakthrough time increased with increasing bed height and decreased with increasing flow rate. The Thomas model as well as the Bed Depth Service Time (BDST) model was fitted to the dynamic flow experimental data to determine the column kinetic parameters useful for designing large-scale column studies. The Thomas model showed good agreement with the experimental results at all the process parameters studied. It could be concluded that TFS may be used as an inexpensive and effective biosorbent without any treatment or any other modification for the removal of Cu(II) ions from aqueous solutions.

Key words: Biosorption, Cu(II), *Tamarindus indica* Fruit Shell, Batch, Fixed-bed Column

INTRODUCTION

In the past few decades, rapid industrialization and unplanned urbanization have resulted in an increased flux of heavy metals into the aquatic environment. The persistence of heavy metals in the aquatic ecosystems have emerged as a severe environmental problem due to their reported toxic and harmful effects towards aquatic life, human beings and the environment [1,2]. Copper is one of the most widely used heavy metals. Copper and its compounds are extensively used in various important industrial applications such as electrical wiring, plumbing, gear wheel, air conditioning tubing, and roofing [3]. Its potential sources in industrial effluents include metal cleaning and plating baths, fertilizer, refineries, pulp, paper board mills, printed circuit board production, wood pulp production, wood preservatives, paints and pigments, municipal and storm water runoff, etc [3-6]. Intake of excessively large doses of copper by human beings leads to severe mucosal irritation and corrosion, stomach upset and ulcer, wide-spread capillary damage, hepatic and renal damage, central nervous system irritation followed by depression, gastrointestinal irritation, and possible necrotic changes in the liver and kidneys [7]. Chronic copper poisoning can also result in Wilson's disease, leading to brain and liver damage [8]. Therefore, removal of copper from effluents is essential not only to protect the water sources but also human health.

Techniques presently in existence for removal of heavy metals from contaminated water bodies include reverse osmosis, electrodialysis, ultrafiltration, ion-exchange, chemical precipitation etc. [9]. However, their practical application is restricted because of technical or economical constraints. Hence, there is a crucial need for a method that will be efficient and cost-effective for the existing contaminated water treatment facilities. In this light, biosorption - the removal of materials (compounds, metal ions, etc.) by inactive, non-living biomass (materials of biological origin) - has been intensively studied worldwide as an efficient and economically sustainable technology for the removal of heavy metals from industrial effluents [1,2]. A number of inexpensive and abundant biosorbents, particularly agricultural waste materials which cost less and can be used as such or after some minor treatment, have been tested and used for removal of heavy metal ions from aqueous solutions [1,10].

Tamarindus indica (Tamarind) is a multipurpose tropical fruit tree grown mainly for its sour fruit pulp [11]. The acidic pulp has a wide variety of domestic and industrial uses [12]. At present, tamarind is cultivated in 54 different countries, with India as the largest producer of tamarind in the world [13]. Its annual production is about 300,000 tons. Tamarind fruit pulp is manufactured and marketed wherever tamarind is cultivated; however, much of the trade is local and carried out in small towns and villages. The seed and the shell are byproducts of the commercial utilization of the fruit and are considered as waste materials with little or no practical value. Utilization of these waste materials as biosorbent is an attractive approach both economically and environmentally. In our previous study, tamarind seeds were shown to be excellent biosorbent for removal of Cu(II) from aqueous media [9]. Therefore, the primary objective of this research was to investigate the Cu(II) biosorption potential of tamarind fruit shell (TFS). Batch experiments were performed to study the effect of various operational parameters such as pH, temperature, contact time, biosorbent dose and initial metal con-

†To whom correspondence should be addressed.
E-mail: chowdhuryshamik@gmail.com

centration on the biosorption process. Equilibrium biosorption data were modeled using Langmuir, Freundlich and Dubinin-Radushkevich (D-R) isotherm models, while the pseudo-first-order, pseudo-second-order and intraparticle diffusion models were used to study the biosorption kinetics. The underlying thermodynamics of the biosorption process was also investigated. To ascertain the practical applicability of the biosorbent for treatment of real industrial wastewaters, fixed-bed column studies were also performed. The effect of important design parameters such as feed flow rate and column bed height was studied using a laboratory scale fixed-bed column. The Thomas model and Bed Depth Service Time (BDST) model were used to analyze the column biosorption data.

MATERIALS AND METHODS

1. Biosorbent

Tamarindus indica fruit shells, used in this study, were collected from the local markets of Durgapur, West Bengal, India. The shells were first washed with distilled water to remove any adhering dust and pulp and dried at 343±1 K for 24 h in an oven. The dried shells were then crushed and ground to fine powder using ball mill and sieved to a constant size (100-125 μm). They were then stored in sterile, closed glass bottles and used as biosorbent without any further pretreatment.

2. Cu(II) Solutions

Stock solution of Cu(II) (500 mg L^{-1}) was prepared by dissolving the required quantity of $CuSO_4 \cdot 5H_2O$ (analytical reagent grade) in double-distilled water. Experimental Cu(II) solution of different concentration was prepared by diluting the stock solution with suitable volume of double-distilled water. The initial pH was adjusted with 0.1 (M) HCl and 0.1 (M) NaOH solutions using a digital pH meter (LI 127, ELICO, India) calibrated with standard buffer solutions.

3. Batch Biosorption Studies

Batch biosorption experiments were carried out in 250 mL glass-stoppered Erlenmeyer flasks with 100 mL of working volume, with Cu(II) concentration of 50 mg L^{-1}. A weighed amount (3 g) of biosorbent was added to the solution. The flasks were agitated at a constant speed of 150 rpm for 4 h in an incubator shaker (Innova 42, New Brunswick Scientific, Canada) at 303±1 K. The influence of pH (2.0, 3.0, 4.0, 5.0, 6.0, 7.0), initial Cu(II) concentration (20, 40, 60, 80, 100 mg L^{-1}), biosorbent dose (0.5, 1, 2, 3, 4, 5 g), contact time (10, 20, 30, 40, 60, 90, 120, 150, 180, 210, 240 min) and temperature (293, 303, 313 K) was evaluated during the present study. Samples were collected from the flasks at predetermined time intervals for analyzing the residual Cu(II) concentration in the solution. The residual amount of Cu(II) in each flask was investigated colorimetrically using UV/VIS spectrophotometer (U-2800, Hitachi, Japan). 1% w/v sodium diethyl dithiocarbamate solution (0.2 mL) and 1.5 N ammonia solution (20 mL) was added to the test sample (1 mL). The absorbance of the resulting yellow colored solution was determined at λ_{max} of 460 nm. The amount of Cu(II) adsorbed per unit TFS (mg metal per g biosorbent) was calculated according to a mass balance on the Cu(II) concentration using Eq. (1):

$$q_e = \frac{(C_0 - C_e)V}{m} \quad (1)$$

The percentage (%) Cu(II) removal was calculated using the following equation:

$$\% \text{ Removal} = \frac{C_0 - C_e}{C_0} \times 100 \quad (2)$$

4. Fixed-bed Biosorption Studies

Continuous flow biosorption experiments were conducted in a glass column (3 cm internal diameter and 50 cm height). TFS was packed into the glass column to yield the desired bed height. A porous sheet was attached at the bottom of the column to support the biosorbent bed and to ensure a good liquid distribution inside the column. The top of the bed was covered by a layer of glass beads (1 mm in diameter) to avoid the loss of biosorbent and also to ensure a closely packed arrangement. Metal solution of known Cu(II) concentration (50 mg L^{-1}) was pumped downward through the column by a peristaltic pump (PP-EX204C, Miclins, India). A series of experiments were conducted to study the effect of feed flow rate (10, 20, 30 mL min^{-1}) and bed height (3, 6 and 12 cm). All the experiments were carried out at pH=6.00 and T=303±1 K. Samples were collected at regular intervals and the concentration of Cu(II) in the effluent was analyzed using a UV/VIS spectrophotometer (U-2800, Hitachi, Japan) as described before. Operation of the column was stopped when the effluent Cu(II) concentration exceeded 99.5% of its initial concentration.

The time for breakthrough appearance and shape of the breakthrough curve are very important for determining the operation and the dynamic response of a biosorption column. Therefore, breakthrough curves, i.e., C_t/C_o vs. time were plotted. The breakthrough time (t_b, the time at which Cu(II) concentration in the effluent reached 1 mg L^{-1}) and bed exhaustion time (t_e, the time at which Cu(II) concentration in the effluent reached 99.5% of initial Cu(II) concentration) were used to evaluate the breakthrough curves.

5. Statistical Analysis

To ensure the accuracy, reliability, and reproducibility of the collected data, all biosorption experiments were performed in triplicate, and the mean values were used in data analysis. Relative standard deviations were found to be within ±3%. Microsoft Excel 2007 program was used for data processing, and linear regression analysis was used to determine the model parameters and constants.

6. Characterization of Biosorbent

6-1. Scanning Electron Microscopy (SEM) Analysis

The surface structure of the biosorbent, before and after biosorption, was analyzed by a scanning electron microscope (S-3000N, Hitachi, Japan) at an electron acceleration voltage of 25 kV. Prior to scanning, the unloaded and Cu(II)-loaded TFS samples were mounted on a stainless steel stab with double stick tape and coated with a thin layer of gold in a high vacuum condition.

6-2. Brunauer-Emmett-Teller (BET) Analysis

The BET surface area, pore volume and pore size of native and metal bound TFS samples were measured by a surface area and porosity analyzer (NOVA 2200, Quantachrome Corporation, USA). A gas mixture of 22.9 mol% nitrogen and 77.1 mol% helium was used for this purpose.

THEORY

1. Biosorption Isotherms

In the analysis and design of a biosorption process, isotherms

provide the most important piece of information for understanding the process. The equation parameters and the underlying thermodynamic assumption of the isotherm models give some idea about the underlying biosorption mechanism as well as the surface properties and affinity of the biosorbent [14]. Therefore, in the present study, the Langmuir, Freundlich, and Dubinin-Radushkevich (D-R) isotherm models were used to describe the equilibrium biosorption data [15].

$$\text{Langmuir: } \frac{C_e}{q_e} = \frac{C_e}{q_m} + \frac{1}{K_L q_m} \tag{3}$$

$$\text{Freundlich: } \log q_e = \log K_F + \left(\frac{1}{n}\right)\log C_e \tag{4}$$

$$\text{Dubinin-Radushkevich (D-R): } \ln q_e = \ln q_m - \beta\varepsilon^2 \tag{5}$$

2. Kinetic Modeling

The knowledge of the kinetics of any biosorption process is crucial in order to be able to design industrial scale separation processes. Therefore, the data obtained from the contact time-temperature dependent experiments were used to study the kinetics of the biosorption process. The pseudo-first-order and pseudo-second-order kinetic models were tested to obtain the rate constants and elucidate the underlying biosorption mechanism [16].

$$\text{Pseudo-first-order: } \log(q_e - q_t) = \log q_e - \frac{k_1}{2.303}t \tag{6}$$

$$\text{Pseudo-second-order: } \frac{t}{q_t} = \frac{1}{k_2 q_e^2} + \frac{1}{q_e}t \tag{7}$$

Since the models mentioned above cannot identify a diffusion mechanism, the intraparticle diffusion model was further used to determine the rate controlling step [17].

$$\text{Intraparticle diffusion: } q_t = k_i t^{0.5} \tag{8}$$

3. Activation Energy and Thermodynamic Parameters

The activation energy E_a for biosorption of Cu(II) by TFS was calculated by the Arrhenius equation [18]:

$$\ln k = \ln A - \frac{E_a}{RT} \tag{9}$$

Thermodynamic behavior of biosorption of Cu(II) by TFS was evaluated by the thermodynamic parameters - Gibbs free energy change (ΔG^0), enthalpy (ΔH^0) and entropy (ΔS^0). These parameters were calculated by using the following equations [19]:

$$\Delta G^0 = -RT \ln K_C \tag{10}$$

$$K_C = \frac{C_a}{C_e} \tag{11}$$

$$\Delta G^0 = \Delta H^0 - T\Delta S^0 \tag{12}$$

4. Modelling of Column Data

The BDST model and Thomas model were fitted to the dynamic flow experimental data to predict the breakthrough curves and to determine the characteristic parameters of the column.

4-1. Thomas Model

The Thomas model is one of the most general and widely used models to describe the behavior of sorption process in fixed-bed columns. The model is based on the assumption that the process follows Langmuir kinetics of sorption-desorption with no axial dispersion [20]. Its main limitation is that its derivation is based on second-order kinetics and considers that sorption is not limited by the chemical reaction but controlled by the mass transfer at the interface [20]. This discrepancy can lead to errors when this method is used to model sorption processes in specific conditions. The model can be described by the following expression [21]:

$$\ln\left[\left(\frac{C_0}{C_t}\right) - 1\right] = \left(\frac{k_{Th} q_0 m}{F}\right) - \left(\frac{k_{Th} C_0 V_{eff}}{F}\right) \tag{13}$$

4-2. BDST Model

The BDST model states that the bed height and service time of a column bear a linear relationship. This model was derived based on the assumption that forces like intra-partcle diffusion and external mass transfer resistance are negligible and that the adsorbate is adsorbed onto the biosorbent surface directly [22]. The BDST model is expressed as [22]:

$$t = \left(\frac{N_0 Z}{C_0 u}\right) - \left(\frac{1}{C_0 k}\right)\ln\left[\frac{C_0}{C_t} - 1\right] \tag{14}$$

RESULTS AND DISCUSSION

1. Characterization of Biosorbent

1-1. SEM Analysis

SEM micrographs of the biosorbent before and after Cu(II) bio-

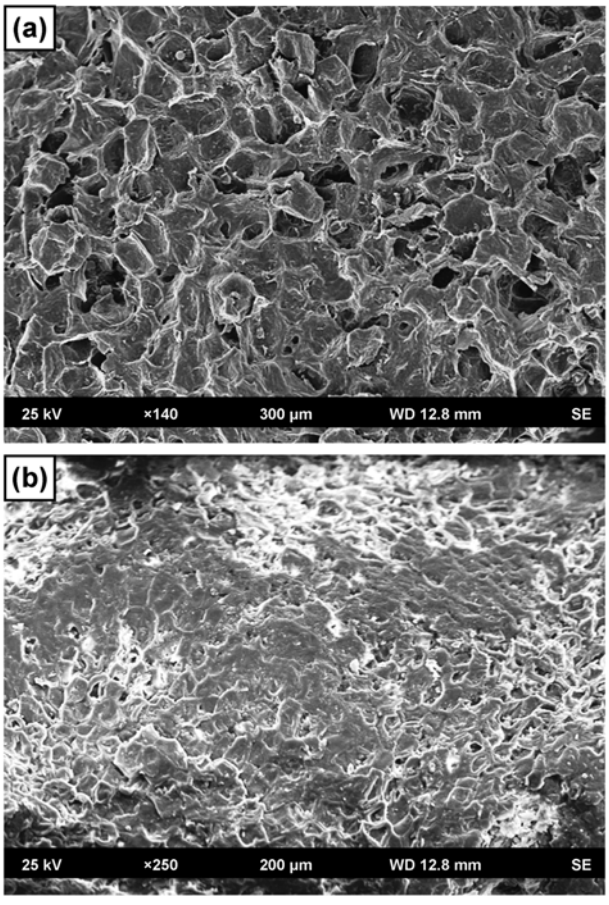

Fig. 1. SEM micrograph of (a) TFS (b) Cu(II) loaded TFS.

sorption are presented in Fig. 1(a)-(b). Before metal uptake, the biosorbent is characterized by irregular and porous structure (Fig. 1(a)). However, as can be seen in Fig. 1(b), the porous textural structure is not observed on the surface of Cu(II)-loaded biosorbent. The surface morphological change can be linked to precipitation/complexation of Cu(II) on the biosorbent surface.

1-2. BET Analysis

The BET surface area, total pore volume and average pore diameter of the biosorbent were found to be 435 $m^2 g^{-1}$, 0.0179 $cm^3 g^{-1}$ and 74 Å, respectively. After Cu(II) biosorption, the BET surface area, total pore volume and average pore diameter of the biosorbent were found to be 471 $m^2 g^{-1}$, 0.0113 $cm^3 g^{-1}$ and 34 Å, respectively. The increase in the surface area of the biosorbent indicates that Cu(II) ions were adsorbed onto the surface of the biosorbent. The decrease in the total pore volume as well as the average pore diameter of the biosorbent suggests that Cu(II) interacts with the functional groups present inside the pores.

2. Batch Studies

2-1. Effect of pH

It is well known that pH is an important monitoring parameter governing biosorption. Thus the effect of pH on the Cu(II) removal efficiency was studied at different pH ranging from 2.0 to 7.0. Since Cu(II) precipitates at pH≥8.0, no further experiments were performed beyond pH 7.0. Results thus obtained are shown in Fig. 2(a). The biosorption efficiency increases with increase in pH of the metal solution, appreciably up to pH 6.0. With further increase in pH, no significant change in metal removal efficiency is observed. Hence all further experiments were carried out at pH 6.0. Similar results were previously reported for biosorption of Cu(II) from aqueous solution onto chestnut shell [7].

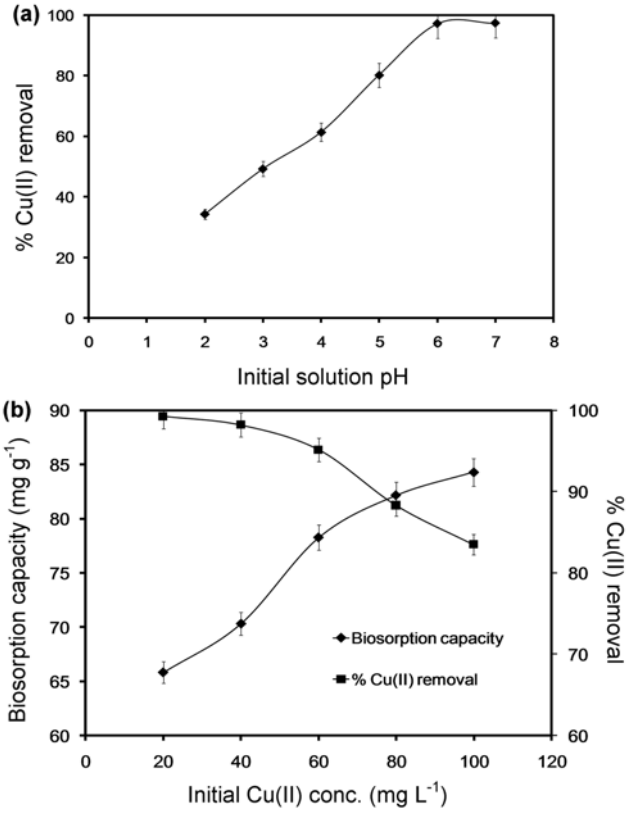

Fig. 2. (a) Effect of pH on biosorption of Cu(II) by TFS (experimental conditions: C_0=50 mg L^{-1}, m=3 g/0.1 L, agitation speed=150 rpm, T=303 K, contact time: 4 h, error bars represent the standard deviation at n=3) (b) Effect of initial Cu (II) concentration on biosorption of Cu(II) by TFS (experimental conditions: pH=6.00, m=3 g/0.1 L, agitation speed =150 rpm, T=303 K, contact time: 4 h, error bars represent the standard deviation at n=3).

TFS mainly contains -OH, -COOH and -CH_2 functional groups on its surface [12]. At low pH values, the surface charge of TFS is positive due to protonation of the surface functional groups. A significant electrostatic repulsion exists between the positively charged surface and the cationic Cu(II) ions, which inhibits the biosorption of Cu(II). Besides, a higher concentration of H^+ in the solution competes with Cu(II) ions for the binding sites of TFS, resulting in reduced uptake. As the pH of the system increases, the number of negatively charged sites on the TFS surface gradually increases due to deprotonation of the functional groups. Obviously, a negatively charged surface site favors the biosorption of cationic Cu(II) ions due to electrostatic attraction. Cu(II) most likely binds on the surface of TFS via ion exchange mechanism according to the following equations:

$$TFS—OH+Cu^{2+} \rightarrow TFS—OCu^{+}+H^{+}$$

$$TFS—COOH+Cu^{2+} \rightarrow TFS—COOCu^{+}+H^{+}$$

where TFS denotes the biosorbent surface.

2-2. Effect of Initial Cu(II) Concentration

The effect of different initial Cu(II) concentration on the biosorption process was also investigated. As illustrated in Fig. 2(b), the biosorption capacity at equilibrium increases from 65.81 to 84.29 mg g^{-1} with increase in initial Cu(II) concentration from 20 to 100 mg L^{-1}. The initial concentration gradient provides an important driving force which helps overcome all mass transfer resistance of Cu(II) ions between the aqueous and solid phases, resulting in an increased biosorption capacity [23]. On the contrary, it can be seen that percentage Cu(II) removal decreases with increase in initial metal ion concentration. At lower concentrations, all Cu(II) ions present in the solution interact with the binding sites of the biosorbent, facilitating about 96% biosorption. However, all biosorbents have a limited number of binding sites, which become saturated at a certain concentration [15]. Hence at higher concentrations, more metal ions are left unadsorbed in the solution due to the saturation of binding sites, resulting in decreased biosorption efficiency. A similar trend was observed for biosorption of Cu(II) by NaOH-modified rice husk [8].

2-3. Effect of Biosorbent Dose

Fig. 3(a) shows the biosorption profile of Cu(II) versus different biosorbent concentration in the range of 0.5 to 5.0 g. It is observed that the Cu(II) removal efficiency increases with increasing biosorbent dose. Such a trend can be attributed to an increase in the sorption surface area and the availability of more sorption sites [18]. Maximum Cu(II) removal (98.17%) is observed at 3.0 g and further increase in biosorbent dose does not significantly change the biosorption yield. This is due to the binding of almost all Cu(II) ions to the biosorbent surface and the establishment of equilibrium between the metal ions on the biosorbent and in the solution [18]. A similar trend has been reported for biosorption of Cu(II) by cotton bolls [23]. All successive batch experiments were performed with a bio-

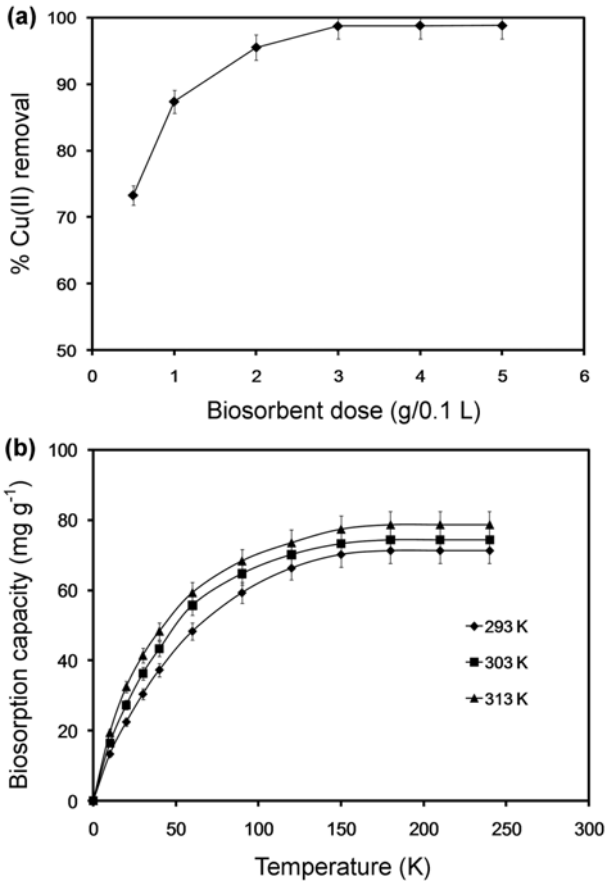

Fig. 3. (a) Effect of biosorbent dose on biosorption of Cu(II) by TFS (experimental conditions: C_0=50 mg L^{-1}, pH=6.00, agitation speed=150 rpm, T=303 K, error bars represent the standard deviation at n=3) (b) Time profiles for biosorption of Cu(II) by TFS at different temperatures (experimental conditions: C_0=50 mg L^{-1}, pH=6.00, m=3 g/0.1 L, agitation speed =150 rpm, error bars represent the standard deviation at n=3).

sorbent dose of 3 g.

2-4. Effect of Temperature and Contact Time

Like pH, temperature is also an important parameter affecting biosorption. The temperature has two main effects. First, increasing temperature is known to increase the diffusion rate of the adsorbate molecules within the pores of the biosorbent as a result of decreasing solution viscosity. Secondly, it will also modify the equilibrium capacity of the biosorbent for a particular adsorbate [24]. Fig. 3(b) shows the biosorption of Cu(II) by TFS at different temperatures as a function of contact time. The Cu(II) binding capacity increases from 71.25 mg g^{-1} to 78.61 mg g^{-1} with rise in temperature from 293 to 313 K at the same metal ion concentration, indicating that Cu(II) removal by biosorption onto TFS was favorable at higher temperatures. The increase in the metal uptake capacity with increasing temperature is either due to the higher affinity of binding sites for Cu(II) or due to an increase in kinetic energy of the biosorbent. An increase in temperature also increases the mobility of the metal ions and decreases the retarding forces acting on the ions. These result in the enhancement in the biosorption capacity of the biosorbent [9]. Cu(II) shows a fast rate of biosorption during the first 90 min of the Cu(II)-biosorbent contact. The fast biosorption rate at the initial stage may be explained by an increased availability in the number of sorption sites on the biosorbent surface [9]. At higher contact time the rate of biosorption tends to slow down, gradually leading to equilibrium. Such behavior can be attributed to the decrease in the number of binding sites available for biosorption. The equilibrium time for maximum Cu(II) uptake is 180 min. After this equilibrium period, the amount of Cu(II) adsorbed does not show time-dependent change. Similar results have been reported in literature for biosorption of Cu(II) by *Tamarindus indica* seed powder [9].

2-5. Biosorption Isotherms

In the present investigation, the isotherm study for biosorption of Cu(II) by TFS was conducted at different temperatures. The Freundlich, Langmuir and D-R isotherm models were used to describe the equilibrium biosorption data. The parameters obtained from the Langmuir (C_e/q_e versus C_e), Freundlich ($\log q_e$ versus C_e) and D-R ($\ln q_e$ versus ε^2) isotherm plots (figures not shown) are listed in Table 1. To quantitatively compare the accuracy of the models, the correlation coefficients (R^2) were also calculated and are listed in Table 1. Analysis of the R^2 values indicates that the Langmuir isotherm model provides the best fit to the equilibrium biosorption data than the other isotherm models. The applicability of the Langmuir isotherm suggests that biosorption took place at specific homogeneous sites within the biosorbent and that once a metal ion occupied a site, no further

Table 1. Isotherm constants and kinetic parameters for biosorption of Cu(II) by TFS at different temperatures

Model	Temperature (K)		
	293	303	313
Isotherm models			
Langmuir			
q_m (mg g^{-1})	73.497	76.387	80.013
K_L (L mg^{-1})	1.467	1.782	1.931
R^2	0.998	0.999	0.999
Freundlich			
K_F (mg g^{-1}) (L $mg^{-1})^{1/n}$	24.784	29.356	33.458
n	3.498	3.972	4.274
R^2	0.952	0.957	0.948
Dubinin-Radushkevich			
q_m (mg g^{-1})	61.821	63.669	65.245
β (mmol^2 J^{-2})	4.26×10^{-9}	4.03×10^{-9}	3.92×10^{-9}
E (kJ mol^{-1})	10.823	11.126	11.281
R^2	0.938	0.931	0.933
Kinetic models			
$q_{e,exp}$ (mg g^{-1})	71.267	74.389	78.624
Pseudo-first-order			
$q_{e,cal}$ (mg g^{-1})	55.104	58. 735	61. 298
k_1 (min^{-1})	4.28×10^{-2}	6.73×10^{-2}	9.68×10^{-2}
R^2	0.921	0.925	0.917
Pseudo-second-order			
$q_{e,cal}$ (mg g^{-1})	72.015	75.183	79.421
k_2 (g mg^{-1} min^{-1})	2.19×10^{-4}	7.03×10^{-4}	1.29×10^{-3}
R^2	0.997	0.995	0.998

biosorption could take place at that site, thereby forming a monolayer [14]. The maximum monolayer biosorption capacity (q_m) increases from 73.49 mg g^{-1} at 293 K to 80.01 mg g^{-1} at 313 K. The Langmuir constant, K_L also increases with increase in temperature. These findings indicate an endothermic nature of the existing process.

The magnitude of the Freundlich constant n gives a measure of favorability of biosorption. Values of n between 1 and 10 represent a favorable biosorption process [17]. For the present study the value of n also presents the same trend at all the temperatures, indicating favorable nature of biosorption of Cu(II) by TFS.

The D-R isotherm model constant β gives an idea about the mean free energy of biosorption E (kJ mol^{-1}) and can be computed using the following relationship [16]:

$$E = \frac{1}{\sqrt{2\beta}} \quad (15)$$

Table 2. Comparison of Cu(II) biosorption capacity of TFS with other reported low-cost biosorbents

Sorbent	pH	Temp (K)	Sorption capacity (mg g^{-1})	Reference
Cinnamomum camphora leaves powder	4.0	303.2	16.75	[25]
		313.2	17.08	
		323.2	17.43	
		333.2	17.87	
NaOH-pretreated *Marrubium globosum* ssp. *globosum* leaves powder	5.5	293	16.23	[26]
Pecan nutshell	5.5	298	85.9	[27]
Tea waste	5.5	295	48.00	[28]
Lentil shell	6.0	293	8.98	[29]
		313	9.51	
		333	9.59	
Wheat shell	6.0	293	7.39	[29]
		313	16.08	
		333	17.42	
Rice shell	6.0	293	1.85	[29]
		313	2.31	
		333	2.95	
Groundnut shell	5.24	308	7.60	[30]
Hazelnut shell activated carbon	6.0	293	48.64	[31]
		303	51.52	
		313	55.40	
		323	58.27	
Rose waste biomass	5.0	303±1	55.79	[32]
Pre-treated arca shell biomass	4.5	298±2	26.88	[33]
Tamarindus indica seed powder	5.5	303	82.97	[9]
		313	100.65	
		323	117.87	
		333	133.24	
Tamarindus indica shell	6.0	293	73.49	Present study
		303	76.72	
		313	80.01	

The magnitude of E may characterize the type of biosorption as chemical ion-exchange (E=8-16 kJ·mol^{-1}) or physisorption (E<8 kJ·mol^{-1}) [16]. In the present study, the values of E were found to be >8 kJ mol^{-1} at all temperatures (Table 1), implying that biosorption of Cu(II) by TFS involves chemical ion-exchange.

A comparative study of the maximum Cu(II) uptake capacity of TFS was performed with other reported sorbents. Note that the maximum amount of metal uptake by various sorbents varies as a function of experimental conditions. Especially, the pH and temperature have a very important effect on the estimation of the maximum amount of metal uptake per unit sorbent. Therefore, for a direct and meaningful comparison, the maximum amount of Cu(II) adsorbed by TFS has been compared to the maximum Cu(II) sorption capacity of other reported sorbents under different experimental conditions (Table 2). In Table 2 the maximum sorption capacity of TFS for Cu(II) is comparable and moderately higher than that of many corresponding sorbent materials. Differences in metal uptake capacity are due to the properties of each sorbent material such as structure, functional groups and surface area. The easy availability and cost effectiveness of TFS are some additional advantages, which make it better biosorbent for treatment of copper wastes.

2-6. Biosorption Kinetics

As already mentioned, the pseudo-first-order and pseudo-second-order kinetic models were used to obtain the rate constants and equilibrium biosorption capacity at different temperatures. The values of the pseudo-first-order model constants, k_1 and q_e, were calculated from the slope and intercept of the plots of log ($q_e - q_t$) versus t, while the pseudo-second-order model constants, k_2 and q_e, were calculated from the slope and intercept of the plots of t/q_t versus t. The calculated model parameters along with the R^2 values are listed in Table 1. The low R^2 values (<0.93) for the pseudo-first-order model indicate that this model is not suitable for describing the biosorption kinetics of Cu(II) onto TFS. However, the relatively high R^2 values (>0.99) for the pseudo-second-order model suggest that the ongoing sorption process obeys pseudo-second-order kinetics. Also, the calculated q_e values ($q_{e,cal}$) show good agreement with the experimental q_e values ($q_{e,exp}$) (Table 1), further confirming that biosorption of Cu(II) by TFS follows the pseudo-second-order kinetic model. The applicability of the pseudo-second-order kinetic model indicates that the biosorption process of Cu(II) onto TFS is chemisorption and the rate-determining step is probably surface biosorption. The pseudo-second-order rate constant, k_2 increases with increase in temperature, suggesting endothermic nature of the existing biosorption process. Similar results have been reported for biosorption of Cu(II) by peanut hull [3].

The possibility of intra-particle diffusion resistance affecting the biosorption process was explored by using the intra-particle diffusion model (Eq. (8)). According to Eq. (8), a plot of q_t versus $t^{0.5}$ should be a straight line passing through the origin when the biosorption mechanism follows the intraparticle diffusion process. However, if the data exhibit multi-linear plots, then the process is governed by two or more steps. The plots for biosorption of Cu(II) by TFS at different temperatures were multimodal with three distinct regions: an initial curve portion followed by a linear portion and then a plateau (Fig. 4). The initial curved region is attributed to the external surface biosorption in which the adsorbate diffuses through the solution to the external surface of the biosorbent. The second

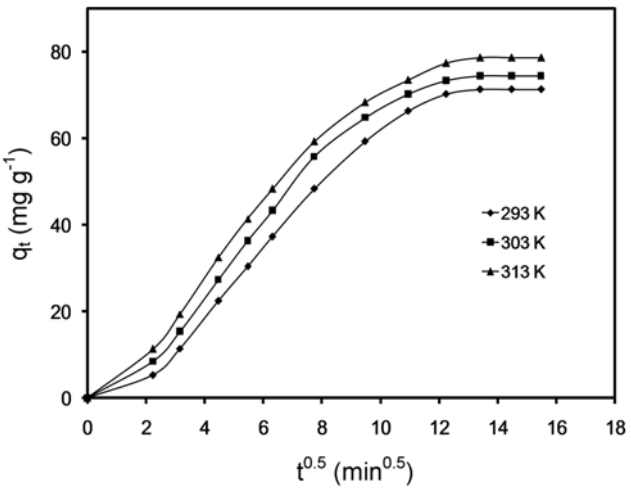

Fig. 4. Weber and Morris plots for biosorption of Cu(II) by TFS at different temperatures (experimental conditions: C_0=50 mg L^{-1}, pH=6.00, m=3 g/0.1 L, agitation speed=150 rpm, contact time: 4 h).

stage relates the gradual uptake reflecting intraparticle diffusion as the rate limiting step. The final plateau region refers to the gradual biosorption stage and the final equilibrium stage, in which the intraparticle diffusion starts to slow down and level out. The present finding implies that although intraparticle diffusion is involved in the biosorption process, it is not the sole rate-controlling step and that some other mechanisms also play an important role. A similar multilinearity was observed for biosorption of Cu(II) by pecan nutshell [27].

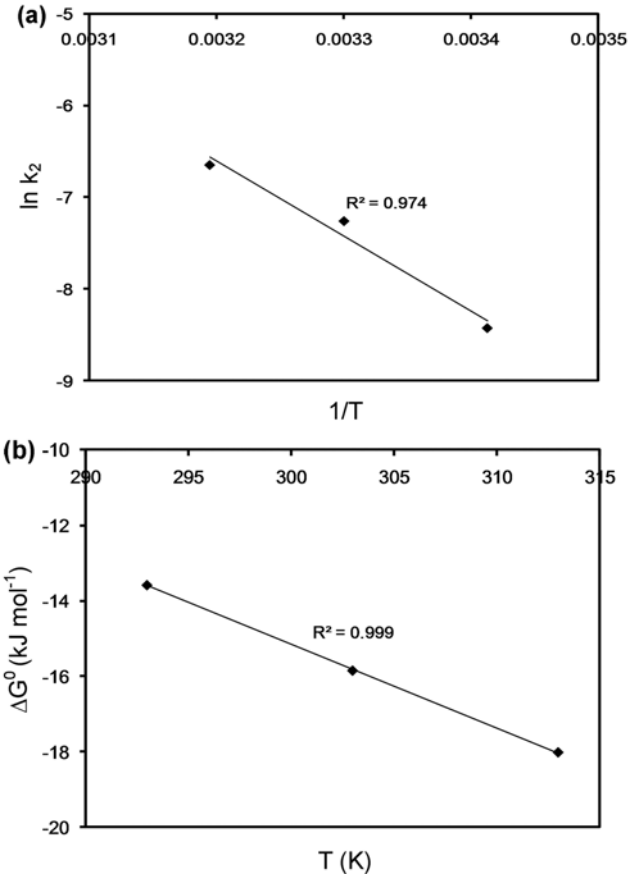

Fig. 5. (a) Arrhenius equation plot for biosorption of Cu(II) by TFS (b) Plot of Gibb's free energy change versus temperature for biosorption of Cu(II) by TFS.

2-7. Activation Energy and Biosorption Thermodynamics

The activation energy for biosorption of Cu(II) by TFS as determined from the slope of the linear plot of $\ln k_2$ versus 1/T (Fig. 5(a)) was 67.93 kJ mol^{-1}. The magnitude of E_a gives information on the nature of the biosorption process, i.e., whether it is physical or chemical, with value of E_a less than 40 kJ mol^{-1} corresponds to physisorption, and higher value represents chemical reaction process [16]. Hence, it can be said that biosorption of Cu(II) by TFS is chemisorption, as already inferred from the D-R isotherm model.

The values of ΔG^0 were estimated using Eq. (10) and were found to be −13.57, −15.85 and −18.01 kJ mol^{-1} at T=293, 303 and 313 K, respectively. The negative value of ΔG^0 at different temperatures indicates the spontaneous nature of the biosorption process. Furthermore, increase in the negative value of ΔG^0 with increasing temperature suggests that the biosorption process is more favorable at higher temperatures. ΔH^0 and ΔS^0 were determined from the intercept and slope of the plot of ΔG^0 versus T (Fig. 5(b)). The value of ΔH^0 was calculated as 51.44 kJ mol^{-1}, and 222.17 J mol^{-1} K^{-1} for ΔS^0. The positive value of ΔH^0 is indicative of the fact that the biosorption reaction is endothermic. The positive value of ΔS^0 reflects the affinity of TFS for Cu(II) ions and an increased randomness at the solid-solution interface during biosorption [33]. It also implies an increase in degree of freedom of the adsorbed species [34]. Similar results have been reported for biosorption of Cu(II) onto palm kernel fiber [35].

3. Column Studies

3-1. Effect of Flow Rate

The effect of flow rate on biosorption of Cu(II) by TFS was studied by varying the flow rate from 10 to 30 mL min^{-1} and keeping the initial Cu(II) concentration (50 mg L^{-1}), pH (6.00) and bed height (5 cm) constant. The breakthrough performance at the above operating conditions is depicted in Fig. 6(a). It can be seen that the breakthrough time as well as the biosorption efficiency is higher at lower flow rates. This can be explained by the fact that at lower flow rate, the residence time of the metal solution is more, and hence the Cu (II) ions get more time to capture the available binding sites around or inside the biosorbent [36]. The metal ions also have more time to diffuse into the pores of the biosorbent through intra-particle diffusion. However, the breakthrough curve becomes steeper when the flow rate increases with which the breakthrough time and the Cu(II) removal efficiency decreases. As the flow rate increases, the residence time of the metal solution in the column decreases and hence the metal ions do not have enough time to capture the binding sites on the biosorbent surface or diffuse into the pores of the biosorbent, leaving the column before equilibrium occurs [37]. A similar trend was previously reported for fixed-bed biosorption of Cu(II) onto sunflower shells [38].

3-2. Effect of Bed Height

To investigate the effect of bed height on the breakthrough curve, metal solution having influent Cu(II) concentration 50 mg L^{-1}, pH 6.0 and flow rate 10.0 mL min^{-1} was passed through the column by varying the bed height. Fig. 6(b) represents the performance of

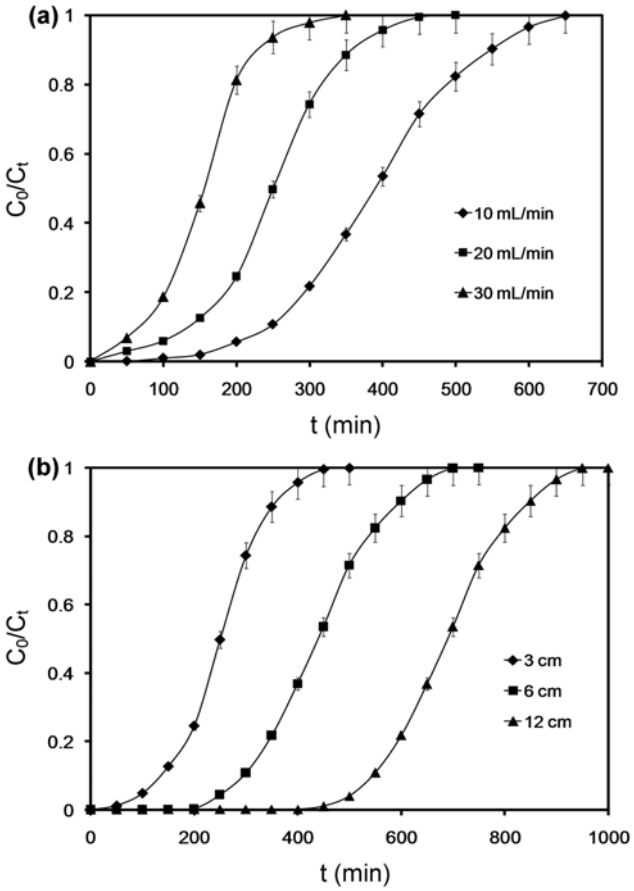

Fig. 6. (a) Effect of flow rate on breakthrough curve (C_0=50 mg L^{-1}, pH=6.00, T=303 K, Z=5 cm, error bars represent the standard deviation at n=3) (b) Effect of bed height on breakthrough curve (C_0=50 mg L^{-1}, pH=6.00, F=10 mL min^{-1}, T=303 K, error bars represent the standard deviation at n=3).

breakthrough curves at bed heights of 3 cm, 6 cm, and 12 cm. As illustrated in Fig. 6(b), the breakthrough time varied greatly with bed height. The breakthrough time increases from 150 min to 550 min, with increase in bed height from 3 to 12 cm. The bed capacity and biosorption efficiency also increases with increasing bed height. As the bed height increases, the metal ions have more time to contact with the biosorbent, resulting in higher Cu(II) removal efficiency [39]. Maximum uptake was observed at the highest bed height due to an increased availability of binding sites for the biosorption process. Such behavior was observed previously by Quek and Al-Duri for biosorption of Cu(II) on coir in a fixed-bed column [40].

3-3. Application of Thomas Model

The experimental data were fitted to the Thomas model to determine the Thomas rate constant (k_{Th}) and bed capacity (q_0). The constants, k_{Th} and q_0, were calculated from the slope and intercept of the plot between $\ln(C_0/C_t-1)$ versus t at different flow rates and bed heights. The calculated values of k_{Th} and q_0 along with the R^2 values are presented in Table 3. The relatively high R^2 values (>0.98) at all the operating conditions suggest that the Thomas model was suitable for describing the column biosorption data of Cu(II) by TFS. The calculated q_o values show good agreement with the experimental q_e values ($q_{e,exp}$), further confirming the suitability of the Thomas model for column design and analysis. The good fit of the experimental data on the Thomas model indicates that the external and internal diffusion were not the rate limiting steps. Based on the q_o values, the maximum Cu(II) uptake capacity is 110.47 mg g^{-1} at the highest bed height of 12 cm and at the minimum flow rate of 10 mL min^{-1}, respectively. This value of column biosorption capacity is significantly high when compared to the biosorption isotherm capacity of 80.01 mg g^{-1}. This difference may be due to the different operating conditions between batch and column experiments [41]. In addition, the dissimilarity between the adsorption capacities might be due to the longer contact time required to reach equilibrium in the adsorption isotherm studies (180 min) compared with the continuous column experiments (<10 min).

3-4. Application of BDST Model

Experimental data obtained from the column studies were further fitted to the BDST model. The values of k and N_0 as estimated from the slope and intercept of the plot of $\ln(C_0/C_t-1)$ versus t at different experimental conditions are given in Table 3. The R^2 values are also listed in Table 3. Analysis of the R^2 values suggests that the BDST model was not suitable for describing the experimental column biosorption data. However, as the bed height increases, the rate constant (k) decreases while the volumetric sorption capacity of the bed (N_0) increases. A reverse trend is observed with increasing flow rate.

4. Desorption and Regeneration Studies

To make the biosorption process more effective and economically feasible, biosorbent regeneration and metal recovery must be evaluated. Desorption of adsorbed Cu(II) ions onto TFS was carried

Table 3. Thomas and BDST model parameters for continuous fixed-bed biosorption of Cu(II) by TFS

Parameter	Thomas				BDST		
	k_{Th} (mL mg^{-1} min^{-1})	q_o (mg g^{-1})	$q_{e,exp}$ (mg g^{-1})	R^2	k (mL mg^{-1} min^{-1})	N_o (mg L^{-1})	R^2
Flow rate (mL min^{-1})							
10	0.6145	103.362	104.013	0.982	0.3826	9489	0.924
20	0.6726	95.278	95.913	0.987	0.4148	8357	0.913
30	0.7253	91.349	92.231	0.985	0.4562	7046	0.917
Bed height (cm)							
3	0.1298	97.378	98.234	0.991	0.3671	8261	0.926
6	0.1337	105.815	106.543	0.986	0.3248	10523	0.922
12	0.1490	109.429	110.472	0.987	0.2917	11786	0.938

out by using 0.5 M HCl, and it was observed that >90% of Cu(II) is desorbed. However, the re-use of TFS was not possible due to its pastry nature after being imbibed in water. The incapability of the regeneration/recycle of the biosorbent would be no severe drawback since the biosorbent is very cheap and readily available.

CONCLUSION

The present study showed that TFS is an effective biosorbent for removal of Cu(II) from aqueous solutions. Operational parameters such as pH, initial metal concentration, biosorbent dose and temperature were found to have an effect on the biosorption efficiency of TFS. Percentage Cu(II) removal decreased with increase in the initial Cu(II) concentration, while it increased with increasing temperature and biosorbent dose. Maximum biosorption was observed at pH 6.0. The biosorption kinetic data showed excellent fit to the pseudo-second-order model indicating chemisorption. Intraparticle diffusion was not the sole rate controlling step. The Langmuir isotherm model provided best fit to the experimental equilibrium data, indicating monolayer sorption on a homogeneous surface. The maximum monolayer biosorption capacity was estimated to be 80.01 $mg \cdot g^{-1}$ at 313 K. According to D-R isotherm model, the Cu(II) biosorption process was chemisorption involving chemical ion-exchange. The calculated thermodynamic parameters indicated endothermic and spontaneous nature of the biosorption process. The maximum Cu(II) biosorption capacity of TFS was comparable and moderately higher than that of many corresponding sorbent materials under quite similar conditions. The breakthrough time increased with increasing bed height, while it decreased with increasing flow rate. The Thomas model showed good agreement with the dynamic flow experimental data. Thus, it can be concluded that TFS should be a promising and cost-effective biosorbent for treatment of copper wastes.

NOMENCLATURE

A : arrhenius constant
C_a : equilibrium Cu(II) concentration on the biosorbent [mg L^{-1}]
C_e : equilibrium Cu(II) concentration in solution [mg L^{-1}]
C_0 : initial Cu(II) concentration [mg L^{-1}]
C_t : Cu(II) concentration in the liquid phase at time t [mg L^{-1}]
E : mean free energy [kJ mol^{-1}]
E_a : activation energy [kJ mol^{-1}]
F : feed flow rate [mL min^{-1}]
ΔG^0 : gibbs free energy change [kJ mol^{-1}]
ΔH^0 : enthalpy of reaction [kJ mol^{-1}]
K_C : distribution coefficient for biosorption
K_F : freundlich constant [mg g^{-1}] (L $g^{-1})^{1/n}$
K_L : langmuir constant [L mg^{-1}]
k : rate constant
K : sorption rate constant [L mg^{-1} min^{-1}]
k_i : intraparticle diffusion rate constant [mg g^{-1} $min^{-0.5}$]
k_{Th} : thomas rate constant [mL mg^{-1} min^{-1}]
k_1 : pseudo-first-order rate constant [min^{-1}]
k_2 : pseudo-second-order rate constant [g mg^{-1} min^{-1}]
m : mass of biosorbent [g]
N_0 : volumetric sorption capacity [mg L^{-1}]
n : freundlich adsorption isotherm constant
q_0 : equilibrium Cu(II) uptake per g of the biosorbent [mg g^{-1}]
q_e : equilibrium Cu(II) uptake per g of the biosorbent [mg g^{-1}]
q_m : maximum biosorption capacity [mg g^{-1}]
q_t : amount of Cu(II) adsorbed at time t [mg g^{-1}]
R : universal gas constant [8.314 J mol^{-1} K^{-1}]
R^2 : correlation coefficient
ΔS^0 : entropy of reaction [J mol^{-1} K^{-1}]
T : temperature [K]
t_b : breakthrough time [min]
t_e : bed exhaustion time [min]
U : linear velocity [cm min^{-1}]
V : volume of the solution [L]
Z : bed height [cm]

Greek Alphabet

β : D-R isotherm constant [$mmol^2$ J^{-2}]
ε : polanyi potential [J $mmol^{-1}$]=RT $\ln(1+1/C_e)$
λ_{max} : wavelength of maximum absorbance

REFERENCES

1. D. Sud, G. Mahajan and M. P. Kaur, *Bioresour. Technol.*, **99**, 6017 (2008).
2. U. Farooq, J. A. Kozinski, M. A. Han and M. Athar, *Bioresour. Technol.*, **101**, 5043 (2010).
3. C. Zhu, L. Wang and W. Chen, *J. Hazard. Mater.*, **168**, 739 (2009).
4. T. S. Anirudhan and P. G. Radhakrishnan, *J. Chem. Thermodyn.*, **40**, 702 (2008).
5. A. Ozer, D. Ozer and A. Ozer, *Process Biochem.*, **39**, 2183 (2004).
6. M. Ajmal, A. H. Khan, S. Ahmad and A. Ahmad, *Water Res.*, **32**, 3085 (1998).
7. Z.-Y. Yao, J.-H. Qi and L.-H. Wang, *J. Hazard. Mater.*, **174**, 137 (2010).
8. H. Jaman, D. Chakraborty and P. Saha, *Clean Soil Air Water*, **37**, 704 (2009).
9. S. Chowdhury and P. D. Saha, *Colloids Surf. B.*, **88**, 697 (2011).
10. A. Demribas, *J. Hazard. Mater.*, **157**, 220 (2008).
11. P. Saha, *Water Air Soil Pollut.*, **213**, 287 (2010).
12. P. Saha, S. Chowdhury, S. Gupta, I. Kumar and R. Kumar, *Clean Soil Air Water*, **38**, 437 (2010).
13. D. Singh, L. Wangchu and S. K. Moond, *Nat. Prod. Rad.*, **6**, 315 (2007).
14. S. Chowdhury, R. Mishra, P. Kushwaha and P. Das, *Biorem. J.*, **15**, 77 (2011).
15. S. Chowdhury and P. Saha, *Chem. Eng. J.*, **164**, 168 (2010).
16. S. Chowdhury, S. Chakraborty and P. Saha, *Colloids Surf. B.*, **84**, 520 (2011).
17. S. Chakraborty, S. Chowdhury and P. D. Saha, *Carbohydr. Polym.*, **86**, 1533 (2011).
18. P. Saha. S. Chowdhury, S. Gupta and I. Kumar, *Chem. Eng. J.*, **165**, 874 (2010).
19. S. Chowdhury, R. Mishra, P. Saha and P. Kushwaha, *Desalination*, **265**, 159 (2011).
20. S. H. Hasan, D. Ranjan and M. Talat, *J. Hazard. Mater.*, **181**, 1134 (2010).
21. M. T. Uddin, M. Rukanuzzaman, M. M. R. Khan and M. A. Islam, *J. Environ. Manage.*, **90**, 3443 (2009).

22. R. Han, D. Ding, Y. Xu, W. Zou, Y. Wang, Y. Li and L. Zou, *Bioresour. Technol.*, **99**, 2938 (2008).
23. H. Duygu Ozsoy and H. Kumbur, *J. Hazard. Mater.*, **136**, 911 (2006).
24. S. Chowdhury and P. Saha, *Sep. Sci. Technol.*, **46**, 1966 (2011).
25. H. Chen, G. Dai, J. Zhao, A. Zhong, J. Wu and H. Yan, *J. Hazard. Mater.*, **177**, 228 (2010).
26. M. Kılıc, H. Yazıcı and M. Solak, *Bioresour. Technol.*, **100**, 2130 (2009).
27. C. P. Vaghetti, E. C. Lima, B. Royer, B. M. da Cunha, N. F. Cardoso, J. L. Brasil and S. L. P. Dias, *J. Hazard. Mater.*, **162**, 270 (2009).
28. B. M. W. P. K. Amarasinghe and R. A. Williams, *Chem. Eng. J.*, **132**, 299 (2007).
29. H. Aydin, Y. Bulut and C. Yerlikaya, *J. Environ. Manage.*, **87**, 37 (2008).
30. S. R. Shukla and R. S. Pai, *Sep. Purif. Technol.*, **43**, 1 (2005).
31. E. Demribas, N. Dizge, M. T. Sulak and M. Kobya, *Chem. Eng. J.*, **148**, 480 (2009).
32. A. R. Iftikhar, H. N. Bhattia, M. A. Hanif and R. Nadeem, *J. Hazard. Mater.*, **161**, 941 (2009).
33. S. Dahiya, R. M. Tripathi and A. G. Hegde, *J. Hazard. Mater.*, **150**, 376 (2008).
34. V. K. Gupta, *Ind. Eng. Chem. Res.*, **37**, 192 (1998).
35. S. Hong, C. Wen, J. He, F. Gan and Y. Ho, *J. Hazard. Mater.*, **167**, 630 (2009).
36. A. E. Ofomaja, *J. Environ. Manage.*, **91**, 1491 (2010).
37. A. Ahmad and B. H. Hameed, *J. Hazard. Mater.*, **175**, 298 (2010).
38. V. Vinodini and N. Das, *Desalination*, **264**, 9 (2010).
39. E. Oguz and M. Ersoy, *Chem. Eng. J.*, **164**, 56 (2010).
40. P. D. Saha, S. Chowdhury, M. Mondal and K. Sinha, *Sep. Sci. Technol.*, **47**, 112 (2011).
41. M. A. Al-Ghouti, M. A. M. Khraisheh, M. N. Ahmad and S. J. Allen, *J. Hazard. Mater.*, **146**, 316 (2007).
42. S. Y. Quek and B. Al-Duri, *Chem. Eng. Process.*, **46**, 477 (2007).